Med Chem Res
DOI 10.1007/s00044-015-1475-9

MEDICINAL CHEMISTRY RESEARCH

ORIGINAL RESEARCH

Fluorine-containing benzothiazole as a novel trypanocidal agent: design, in silico study, synthesis and activity evaluation

Roberto I. Cuevas-Hernández[1] · José Correa-Basurto[1] · César A. Flores-Sandoval[2] · Itzia I. Padilla-Martínez[3] · Benjamín Nogueda-Torres[4] · María de Lourdes Villa-Tanaca[4] · Feliciano Tamay-Cach[1] · Juan J. Nolasco-Fidencio[1] · José G. Trujillo-Ferrara[1]

Received: 19 May 2015 / Accepted: 26 September 2015

Abstract *Trypanosoma cruzi* (*T. cruzi*) is the etiologic agent of Chagas disease. In the bloodstream of humans, this parasite is in the trypomastigote stage and can infect host cells. Its metabolism is dependent on the glycolysis pathway, and one enzyme important for the optimal functioning of this metabolic pathway is triosephosphate isomerase (TIM). The significant difference (48 %) between the interfacial residues of TIMs from humans and trypanosomes and the importance of these residues for the stability of *T. cruzi* TIM (TcTIM) make this enzyme a possible therapeutic target. In the present study, 204 benzazole derivatives were designed as TcTIM inhibitors, including some well-known ligands. Compounds were analyzed with docking simulations and a QSAR study, and their molecular physicochemical properties were calculated. The five compounds selected from in silico screening were later synthesized and assayed in vitro for their trypanocidal activity on a resistant strain of *T. cruzi*. All compounds showed affinity for the aromatic cluster of the TcTIM interface, with important electrostatic, hydrophobic and π–π interactions. The benzothiazole derivatives had better physicochemical attributes than the currently prescribed drug, benznidazol. Although **BT1**and **BT2** showed toxicity problems, **BT3** did not. The QSAR study indicates that the inhibition of TcTIM improves when the compounds (especially benzothiazoles) are substituted with hyper-conjugated systems and there is a sulfur atom in their structure. It was found with in vitro assays that compound **BT3** is a better trypanocidal agent than the currently used drug on the market for the treatment of Chagas disease, benznidazol.

Keywords Anti-trypanosomal drug · Docking simulation · Fluorine-containing benzothiazole · *T. cruzi* · Triosephosphate isomerase · Trypanocidal activity · Quantitative structure–activity relationship

Electronic supplementary material The online version of this article (doi:10.1007/s00044-015-1475-9) contains supplementary material, which is available to authorized users.

✉ Roberto I. Cuevas-Hernández
rcuevash@ipn.mx

✉ José G. Trujillo-Ferrara
jtrujillo@ipn.mx

José Correa-Basurto
corrjose@gmail.com

César A. Flores-Sandoval
caflores@imp.mx

Itzia I. Padilla-Martínez
ipadillamar@ipn.mx

Benjamín Nogueda-Torres
bnogueda@hotmail.com

María de Lourdes Villa-Tanaca
loudesvilla@hotmail.com

Feliciano Tamay-Cach
dr.felicianotamay@gmail.com

Juan J. Nolasco-Fidencio
jesusprestige@hotmail.com

[1] Departamento de Bioquímica, Laboratorio de Modelado molecular y Bioinformática, Escuela Superior de Medicina, Instituto Politécnico Nacional, 11340 Mexico, D.F., Mexico

[2] Instituto Mexicano del Petróleo, 07730 Mexico, D.F., Mexico

[3] Unidad Profesional Interdisciplinaria de Biotecnología, Instituto Politécnico Nacional, 07340 Mexico, D.F., Mexico

[4] Departamento de Parasitología y Departamento de Microbiología, Escuela Nacional de Ciencias Biológicas, Instituto Politécnico Nacional, 11340 Mexico, D.F., Mexico

Published online: 15 October 2015

Introduction

Chagas disease is a type of trypanosomiasis caused by the protozoan parasite *Trypanosoma cruzi* (*T. cruzi*). It constitutes the greatest threat to public health in the parts of Latin America that suffer from widespread poverty. *T. cruzi* proliferates in communities where houses have dirt floors and adobe walls. This parasite progressively invades human cells and lyses them in order to multiply and spread, and as a result causes chronic incurable complications such as Chagasic cardiomyopathy as well as damage to the gastrointestinal tract and peripheral neurological lesions (Rassi Jr. *et al.*, 2010; Marin *et al.*, 2007). An estimated 8 million people are infected with *T. cruzi* in Latin America, the Caribbean and the Southern United States. Due to the increasing mobility of people in the world, this parasite has now spread to other continents (WHO, 2015), and today more than 100 million people are considered to be at risk for this disease (OPS, 2006). A parasite related to *T. cruzi* has been found in Africa (causing sleeping sickness) and Asia (causing human Asian trypanosomiasis).

The drugs currently available for treating this disease are ineffective or have serious collateral effects. One strategy for drug design is based on targeting the metabolism of *T. cruzi*, which obtains its energy from the glycolysis pathway. The key to this strategy is the identification of enzymes that are distinct between *T. cruzi* and humans and therefore can be targeted to selectively inhibit the parasite without side effects for patients (Verlinde *et al.*, 2001). One such enzyme is triosephosphate isomerase (TIM), which catalyzes the interconversion of dihydroxyacetone phosphate (DHAP) into *R*-glyceraldehyde-3-phosphate (G3P) in parasites and humans (Knowles, 1991), leading to energy from glycolysis.

TIM from *T. cruzi* (TcTIM) is a well-known dimeric enzyme (Banner *et al.*, 1975; Lolis and Petsko, 1990; Maldonado *et al.*, 1998) whose crystal structure is available in the protein data bank (PDB) with the code 1TCD (http://www.rcsb.org/pdb/home/home.do). Several studies have shown the structure–activity relationship of TIM (Zomosa *et al.*, 2003; Olivares *et al.*, 2007), as well as the significant difference of 48 % between the interfacial residues of TIM from humans and parasites (Garza *et al.*, 1998; Saab *et al.*, 2011). Recently, it has been demonstrated that a good strategy for drug design is to seek inhibitors of the aromatic cluster of residues present in the TcTIM dimer interface (as well as in other TIMs from distinct parasite species) (Espinoza and Trujillo, 2004, 2005, 2006; Espinoza *et al.*, 2010; Alvarez *et al.*, 2010; Romo *et al.*, 2011; Flores *et al.*, 2013).

The aim of the present study was to rationally design a series of 204 molecules as TcTIM inhibitors, which included some well-known ligands. These structurally related compounds were first evaluated with in silico tools in order to establish a model structure. QSAR was assessed with molecular modeling, physicochemical descriptors and docking simulations. Possible toxicity was also analyzed using Web databases. Taking into account this in silico screening, a new molecule was designed with the features needed to inhibit TcTIM, while another two were formed in order to validate our model. In the end, five compounds among the series were synthesized and tested in vitro for possible trypanocidal activity.

Materials and methods

Computational studies

The structures of target compounds were fully optimized at the B3LYP/6-31G(*d*) level, implemented in Gaussian 03 software (Frisch *et al.*, 2003). Some QSAR descriptors included in Hyperchem software were taken into account from optimized structures. The training model was built using stepwise subroutine multiple lineal regression (MLR) (Xu *et al.*, 2012) of the SPSS for Windows version 13.0. (SPSS, 1999). The optimization of the linear models was determined by considering the t-statistical models (with all absolute values >2.0 accepted) as well as the overall *F*-statistical test. We also performed Akaike's Information Criterion (AIC) (Akaike, 1974; Guha and Jurs, 2005).

Docking simulations were carried out by using AutoDock 4.0.1 (Morris *et al.*, 1998) and AutoDock tools 1.5.4 (Sanner, 1999). The specific conditions of interaction between the ligands and the biological receptor (TcTIM) were established by taking the crystallographic coordinates of the Protein Data Bank. Before docking, water molecules were removed from TcTIM and hydrogen atoms were added to the polar atoms, considering a ~7.4 pH value and taking into account the Kollman charges for all atoms in the receptor. The other parameters were left at their default values. Finally, the whole protein was minimized in the Nanoscale Molecular Dynamics (NAMD 2.6) program using the CHARMM27 force field, and water molecules were added using the Visual Molecular Dynamics (VMD v.1.8.6) program (Phillips *et al.*, 2005; Humphrey *et al.*, 1996).

To identify binding modes, all the possible rotatable bonds, torsion angles, atomic partial charges, and merge non-polar hydrogens of the ligands were assigned. Binding modes were then docked on the interdimeric enzyme surface, using a grid box of 60 × 100 × 60 Å, a grid spacing of 0.375 Å, and the following grid center: $X = 13.341$, $Y = 50.553$ and $Z = 55.738$. The hybrid Lamarckian Genetic Algorithm was used, with an initial

population of 100 randomly placed individuals and a maximum number of energy evaluations of 107. All other parameters were left at their default settings. The resulting docked orientations within a root-mean-square deviation of 0.5 Å were clustered together, and the lowest energy cluster returned by AutoDock for each compound was used for further analysis. All ligand–enzyme complexes were visualized by VMD v.1.8.6 and Discovery Studio 4.0 (Dassault Systèmes, 2015) programs.

Validation parameters

One of the most commonly applied internal validation techniques is the leave-one-out cross-validation (LOO-CV). The measurements connected to internal validation by LOO-CV (q^2_{cv}) are defined as follows:

$$q^2_{cv} = 1 - \frac{\sum_{i=1}^{n}\left(y_i^{obs} - y_i^{predcv}\right)^2}{\sum_{i=1}^{n}\left(y_i^{obs} - \bar{y}_i^{obs}\right)^2} \quad (1)$$

where y_i^{obs} is the experimental (observed) value of the property for the *i*th compound; y_i^{predcv} is the predicted value for the temporary excluded (cross-validated) *i*th compound; $\bar{y}_i^{obs}$ is the mean experimental value of the property in the training set; and n is the number of compounds in the training set. Cross-validation provides a reasonable approximation of the ability of QSAR to predict the activity values of new compounds. However, external validation gives the ultimate proof of the true predictability of a model. In this sense, to achieve a better external predictive potential of the model, a modified $r^2_{m(test)}$ was introduced with the following equation (Roy and Roy, 2008; Roy *et al*., 2009):

$$r^2_{m(test)} = r^2 \times \left(1 - \sqrt{r^2 - r_0^2}\right) \quad (2)$$

where r^2 is the squared correlation coefficient between observed and predicted values, and r_0^2 is the squared correlation coefficient between the observed and predicted values with the intercept set at zero. The value of $r^2_{m(test)}$ should be greater than 0.5 to be acceptable. Moreover, this value may be used for selection of the best predictive models among comparable models.

General procedure for synthesis of benzothiazole and benzoxazole derivatives

Five compounds were synthesized, including three benzothiazoles (**BT1**, **BT2** and **BT3**) obtained by modifying the reaction conditions described elsewhere (2011) (Scheme 1) and two benzoxazoles (**C***fad*3 and **C***fad*5, according to a previously described method) (Trujillo *et al.*, 2004).

The appropriate 2-aminothiophenol was mixed with a substituted benzaldehyde (both previously dissolved in 5 mL of DMSO anh.) and an equimolar amount of $Na_2S_2O_5$. DMSO was then added to attain 30 mL of mixture, which was stirred at reflux at ~120 °C for 40 min. The desired compound was monitored by TLC analysis (using Ethyl acetate as eluent). The mixture was cooled to room temperature by adding cool water, and the resulting precipitate was collected by vacuum filtration. The filtrate was then washed with an excess of water and left to dry. The resulting powder was dissolved in CH_2Cl_2 (70 mL), and the remaining traces of sodium metabisulfite were extracted with brine (70 mL) and solvent removed under vacuum. The resulting product was purified and recrystallized in ethanol/water (1:3) with activated carbon to obtain mostly white needles.

Chemical characterization

The reactions were monitored by TLC and all synthesized compounds were characterized by ^1H,^{13}C NMR (300 MHz) spectra on a Jeol GSX-300 spectrometer using DMSO-d_6 as solvent and TMS as internal reference. Chemical shift values (δ_{ax}) are in parts per million (ppm), and coupling constants (*J* values) are in Hertz (Hz). ESI–MS were recorded on a Bruker micrOTOF-Q II. Infrared spectra (IR) were obtained with a MIDAC M2000 FT-IR spectrophotometer using KBr pellets. The uncorrected melting points were obtained in open-ended capillary tubes in an Electrothermal 9300 digital apparatus.

2-phenyl-1,3-benzothiazole (**BT1**) 2-aminothiophenol (14.62 mmol) and benzaldehyde (14.96 mmol) were reacted to give a compound as white needles, 77 % yield, mp = 95–96 °C; IR (KBr, cm^{-1}) ν: 3064 (C-HAr), 1432 (C=N), 684 (C-S); ^1H NMR: δ 7.49 (H-7), 7.56 (H-12, H-13, H-14, H-8), 8.06 (H-6), 8.08 (H-11, H15), 8.1 (H-9); ^{13}C NMR: δ 167.99 (C-2), 154.23 (C-4), 135.12 (C-5), 133.52 (C-10), 132.13.42 (C-13), 130.10 (C-12, C-14), 127.88 (C-11, C-15), 127.37 (C-7), 126.26 (C-8), 123.58 (C-6), 123.06 (C-9). *m/z* (ESI) 212.05 [M^+].

4-(1,3-benzothiazol-2-yl)benzoic acid (**BT2**) 2-Aminothiophenol (2.6 mmol) and 4-Formylbenzoic acid (2.8 mmol) were reacted to give a compound as a white powder, 63 % yield, mp = 332 °C; IR (KBr, cm^{-1}) ν: 3059 (C-HAr), 1684 (COOH), 1425 (C=N), 689 (C-S); ^1H NMR: δ 7.49 (H-7, dd, J = 11.8), 7.55 (H-8, dd, J = 12), 8.07 (H-6, s), 8.10 (H-12, H15, s), 8.18 (H-11, H-14, s), 8.20 (H-9, s); ^{13}C NMR: δ 167.36 (C-16), 166.85 (C-2), 154.18 (C-4), 137.01 (C-5), 135.42 (C-10), 133.81 (C-13), 130.96 (C-11, C-15), 128.0 (C-12, C-14), 127.58 (C-8), 126.67 (C-7), 123.87 (C-6), 123.22 (C-9); *m/z* (ESI) 254.0341 [M^+].

Scheme 1 Synthesis pathway for benzothiazole derivatives

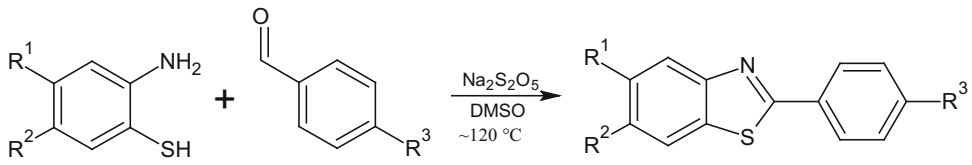

BT1) $R^1 = R^2 = R^3 = H$
BT2) $R^1 = R^2 = H$, $R^3 = COOH$
BT3) $R^1 = CF_3$, $R^2 = H$, $R^3 = COOH$

4-[5-(trifluoromethyl)-1,3-benzothiazol-2-yl]benzoic acid (**BT3**) 2-Amino-4-(trifluoromethyl)benzenethiol (7.31 mmol) and 4-Formylbenzoic acid (7.48 mmol) were reacted to give a compound as a white flaky crystal, 51 % yield, mp = 258–260 °C; IR (KBr, cm^{-1}) ν: 3068 (C-HAr), 1686 (COOH), 1141 (C-F_3), 691 (C-S); ^{1}H NMR: δ 7.81 (H-7, d, $J = 8.4$), 8.12 (H-11, H-15 $J = 8.4$), 8.23 (H-12, H-14 $J = 8.4$), 8.45 (H-6, d, $J = 7.8$), 8.45 (H-9, s), 13.35 (H-17); ^{13}C NMR: δ 167.36 (C-17), 166.85 (C-2), 154.18 (C-4), 137.01 (C-10), 135.42 (C-5), 133.81 (C-13), 130.96 (C-11, C-15), 128.0 (C-12, C-14), 127.58 (C-8), 126.67 (C-7), 123.87 (C-6), 123.22 (C-9), *m/z* (ESI) 322.0214 [M^+].

(2E)-3-(1,3-benzoxazol-2-yl)prop-2-enoic acid (**C***fad5*) Brown crystals, 70 % yield, mp = 227–229 °C; IR (KBr, cm^{-1}): ν 1710 (COOH), 1527 (C=N); ^{1}H NMR: δ 6.92 (H-11, d, $J_{trans} = 15.8$), 7.45 (H-10, d, $J_{trans} = 15.9$), 7.77 (H-7, d, $J_o = 8.6$), 7.52 (H-6, d, $J_o = 8.6$), 7.44 (H-5, d, $J_o = 8.6$) 7.84 (H-4, br); ^{13}C NMR: δ 166.0 (C-12), 159.9 (C-2), 150.1 (C-8), 141.4 (C-9), 129.3 (C-11), 128.2 (C-10), 126.9 (C-6), 125.2 (C-5), 120.5 (C-4), 111.1 (C-7); *m/z* (ESI) 190.0411 [M^+].

(2E)-3-(6-methyl-1,3-benzoxazol-2-yl)prop-2-enoic acid (**C***fad3*) Light brown powder, 42 % yield, mp = 238–239 °C; IR (KBr, cm^{-1}) ν: 1710 (COOH), 1544 (C=N); ^{1}H NMR: δ 2.44 (H-4, s), 6.83 (H-11, d, $J_{trans} = 15.9$), 7.37 (H-10, d, $J_{trans} = 15.9$), 7.67 (H-7, d, $J_o = 8.0$), 7.23 (H-5, d, $J_o = 8.0$), 7.5 (H-4, br); ^{13}C NMR: δ 166.5 (C-12), 129.1 (C-10), 128.7 (C-11), 159.8 (C-2), 150.8 (C-9), 137.8 (C-8), 120.3 (C-7), 127.0 (C-6), 139.7 (C-5), 111.5 (C-4); *m/z* (ESI) 204.0594 [M^+].

In vitro susceptibility assays

For this study, a *T. cruzi* strain, INC-5, was isolated from chronic Chagas patients of an endemic area of Mexico. The *T. cruzi* stock strains were routinely maintained in triatomine bugs (Meccus longipennis) and periodically passed through albino mice.

The methodology employed was carried out according to the protocol reported elsewhere (Díaz *et al.*, 2011). At the peak of parasitemia, bloodstream trypomastigotes were obtained by cardiac puncture from male NIH mice. 195 µL of blood with 2×10^5 trypomastigotes was placed in each well of sterile 96-well plates. Five microliters of one of the concentrations of compounds (**C***fad5*, **C***fad3*, **BT1**, **BT2** or **BT3**) was added to obtain a final concentration (5, 10, 50 or 100 µmol/mL). The final concentration of DMSO in the culture medium remained below 1 %. A solution of DMSO/H_2O (1:99) was used as the negative control and 12.5 µmol/mL crystal violet as the positive control (100 % lysis). The plates were incubated at 4 °C for 24 h. Bloodstream trypomastigotes were counted in a Neubauer chamber. The trypanocidal effect was determined by comparing the remaining trypomastigotes in each concentration with the negative control group. Stock solutions (10 µmol/mL) of each test compound and reference drugs were prepared in DMSO, and subsequent dilutions were made with sterile distilled water. Each assay was performed in triplicate.

Results and discussion

Molecular modeling and docking studies

Two hundred and four potential ligands were designed based on the lead compound, benzazole, with the aim of exploring different electronic effects. Derivatives were formed by substituting the benzazole ring at position C6 or C7 with functional groups commonly found in organic molecules. These compounds were divided into three families according to the expected electronic effects. In the benzazole ring there were compounds with N–NH (benzimidazoles), N–S (benzothiazoles) and N–O (benzoxazoles). The electronic effects were evaluated with the Hammett constants ($\sigma_{\rho,m}$) in order to establish whether a given derivative is electron withdrawing or donating (Hansch *et al.*, 1991). These derivatives were also substituted at the C2 position to elongate the chain (including unsaturated systems in *cis* and *trans* configurations) in order to observe lipophilic and steric effects (Table 1). All

Table 1 Chemical structure of benzazole derivatives

Lead compound

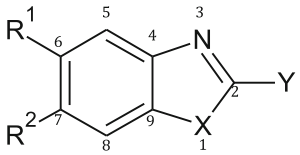

Heteroatom in the azole ring (X = Family)	Substituent at C2 (Y = series)	Aromatic ring substituent at C6 or C7		
		R^1	R^2	σ^a
A=NH (benzimidazole)	*bad* = $-(CH_2)_3CO_2H$	1 = H	NH_2	−0.66
		2 = H	OH	−0.37
	fad = $-(CH)_2CO_2H$ (*E*) configuration	3 = H	CH_3	−0.17
		4 = H	CH_2CH_3	−0.15
B=S (benzothiazole)	*mad* = $-(CH)_2CO_2H$ (*Z*) configuration	5 = H	H	0.00
		6 = H	F	0.06
C=O (benzoxazole)	*pad* = $-(CH_2)_2CO_2H$	7 = H	Cl	0.23
		8 = H	COOH	0.45
		9 = H	NO_2	0.78
		10 = NH_2	H	−0.16
		11 = OH	H	0.12
		12 = CH_3	H	−0.07
		13 = CH_2CH_3	H	−0.07
		14 = F	H	0.34
		15 = Cl	H	0.37
		16 = COOH	H	0.37
		17 = NO_2	H	0.71

Each derivative is formed from the lead compound and involves a substitution at position 1 with heteroatom NH (**A**), S (**B**) or O (**C**) to give a total of three benzazole families (benzimidazole, benzothiazole and benzoxazole). A substitution was then made at the C2 position with the fragments derived from butanoic acid (*bad*), propionic acid (*pad*), fumaric acid (*fad*) and maleic acid (*mad*) to give a total of four series for each of the three families, resulting in 12 series. For each series, there was a substitution at position C6 or C7 to give a total of 17 combinations, resulting in a total of 204 combinations. For example, compound **B***fad*12 corresponds to family **B** (benzothiazole), the *fad* series (a fumaric acid moiety at the C2 position) and 12 corresponds to a substitution at $R^1 = CH_3$ and $R^2 = H$

[a] σ_p *or* σ_m = Hammett constants

compounds were geometrically optimized at the B3LYP/6-31G(*d*) level.

The target compounds were docked on the interface of the two monomers of the enzyme. According to the in silico results, compound **B***bad*9 of the family of benzothiazoles showed the greatest affinity for TcTIM, with a $\Delta G = -5.25$ kcal/mol. The binding energies for ligand–enzyme complexes for each of the families of benzazoles are shown in Tables 2, 3 and 4. The compounds with the highest affinity for TcTIM are those containing electron-withdrawing groups on the benzazole ring. These results are consistent with the high electron density present in the interfacial region of TcTIM.

Molecular physicochemical properties

Although docking simulations provide a powerful tool for selecting molecules with a certain structure, it is necessary to consider other theoretical tools to estimate pharmacological activity. By using programs available on line, important pharmacological properties can be taken into account, including absorption, bioavailability, permeability, blood–brain barrier penetration, metabolism and excretion. All of these properties should be taken into account to achieve greater affinity for the biological receptor, lower toxicity and better scores according to

Table 2 ΔG values in Kcal/mol for the benzimidazole derivatives

Compound	ΔG	Compound	ΔG	Compound	ΔG	Compound	ΔG
A*bad*1	−4.80	**A***mad*1	−4.19	**A***fad*1	−4.24	**A***pad*1	−4.10
A*bad*2	−4.74	**A***mad*2	−4.50	**A***fad*2	−4.11	**A***pad*2	−4.25
A*bad*3	−4.40	**A***mad*3	−3.77	**A***fad*3	−3.97	**A***pad*3	−4.61
A*bad*4	−4.55	**A***mad*4	−4.45	**A***fad*4	−3.89	**A***pad*4	−4.59
A*bad*5	−4.26	**A***mad*5	−3.62	**A***fad*5	−3.80	**A***pad*5	−3.74
A*bad*6	−4.01	**A***mad*6	−3.40	**A***fad*6	−3.75	**A***pad*6	−3.63
A*bad*7	−4.62	**A***mad*7	−3.96	**A***fad*7	−4.00	**A***pad*7	−4.68
A*bad*8	−4.83	**A***mad*8	−4.30	**A***fad*8	−3.50	**A***pad*8	−3.77
A*bad*9	−5.18	**A***mad*9	−4.64	**A***fad*9	−3.73	**A***pad*9	−4.22
A*bad*10	−4.64	**A***mad*10	−4.67	**A***fad*10	−4.15	**A***pad*10	−4.00
A*bad*11	−4.61	**A***mad*11	−4.01	**A***fad*11	−4.13	**A***pad*11	−4.44
A*bad*12	−4.52	**A***mad*12	−4.28	**A***fad*12	−3.99	**A***pad*12	−4.06
A*bad*13	−4.53	**A***mad*13	−4.32	**A***fad*13	−3.9	**A***pad*13	−4.72
A*bad*14	−4.15	**A***mad*14	−4.11	**A***fad*14	−3.74	**A***pad*14	−3.65
A*bad*15	−4.46	**A***mad*15	−3.84	**A***fad*15	−4.02	**A***pad*15	−4.11
A*bad*16	−4.65	**A***mad*16	−3.91	**A***fad*16	−3.65	**A***pad*16	−4.00
A*bad*17	−4.86	**A***mad*17	−4.28	**A***fad*17	−3.84	**A***pad*17	−4.05

Table 3 ΔG values in Kcal/mol for the benzothiazole derivatives

Compound	ΔG	Compound	ΔG	Compound	ΔG	Compound	ΔG
B*bad*1	−5.01	**B***mad*1	−4.64	**B***fad*1	−4.58	**B***pad*1	−4.75
B*bad*2	−5.00	**B***mad*2	−4.42	**B***fad*2	−4.27	**B***pad*2	−4.53
B*bad*3	−4.58	**B***mad*3	−4.10	**B***fad*3	−4.32	**B***pad*3	−4.6
B*bad*4	−4.58	**B***mad*4	−4.12	**B***fad*4	−4.29	**B***pad*4	−4.64
B*bad*5	−4.44	**B***mad*5	−3.91	**B***fad*5	−4.15	**B***pad*5	−4.36
B*bad*6	−4.31	**B***mad*6	−3.86	**B***fad*6	−4.11	**B***pad*6	−4.33
B*bad*7	−4.61	**B***mad*7	−4.1	**B***fad*7	−4.37	**B***pad*7	−4.68
B*bad*8	−4.7	**B***mad*8	−4.71	**B***fad*8	−3.78	**B***pad*8	−4.16
B*bad*9	−5.25	**B***mad*9	−4.82	**B***fad*9	−3.91	**B***pad*9	−4.38
B*bad*10	−5.07	**B***mad*10	−4.54	**B***fad*10	−4.52	**B***pad*10	−4.8
B*bad*11	−4.82	**B***mad*11	−4.33	**B***fad*11	−4.48	**B***pad*11	−4.7
B*bad*12	−4.66	**B***mad*12	−4.12	**B***fad*12	−4.29	**B***pad*12	−4.64
B*bad*13	−4.67	**B***mad*13	−4.28	**B***fad*13	−4.28	**B***pad*13	−4.65
B*bad*14	−4.35	**B***mad*14	−3.9	**B***fad*14	−4.57	**B***pad*14	−4.27
B*bad*15	−4.7	**B***mad*15	−4.17	**B***fad*15	−5.00	**B***pad*15	−4.75
B*bad*16	−4.94	**B***mad*16	−4.88	**B***fad*16	−3.77	**B***pad*16	−4.68
B*bad*17	−5.23	**B***mad*17	−4.69	**B***fad*17	−4.2	**B***pad*17	−4.99

Lipinski's Rules (Lipinski *et al.*, 2001) and the contribution of Veber *et al.*, (2002).

These molecular physicochemical properties were calculated for all ligands under study, particularly for the six compounds reported elsewhere as possible inhibitors of TcTIM (Alvarez *et al.*, 2010; Flores *et al.*, 2013). The descriptors obtained with molinspiration cheminformatics (2015) and OSIRIS Property Explorer (Organic Chemistry Portal, 2015) were the number of hydrogen bond acceptors (N_{hba}) and hydrogen bond donors (N_{hbd}), the number of

Table 4 ΔG values in Kcal/mol for the benzoxazole derivatives

Compound	ΔG	Compound	ΔG	Compound	ΔG	Compound	ΔG
C*bad*1	−4.7	**C***mad*1	−4.71	**C***fad*1	−4.38	**C***pad*1	−4.46
C*bad*2	−4.6	**C***mad*2	−4.5	**C***fad*2	−4.26	**C***pad*2	−4.44
C*bad*3	−4.38	**C***mad*3	−4.26	**C***fad*3	−4.03	**C***pad*3	−4.35
C*bad*4	−4.37	**C***mad*4	−4.14	**C***fad*4	−4.06	**C***pad*4	−4.42
C*bad*5	−4.18	**C***mad*5	−3.83	**C***fad*5	−3.92	**C***pad*5	−4.1
C*bad*6	−4.11	**C***mad*6	−3.8	**C***fad*6	−3.83	**C***pad*6	−4.02
C*bad*7	−4.42	**C***mad*7	−4.22	**C***fad*7	−4.08	**C***pad*7	−4.46
C*bad*8	−4.70	**C***mad*8	−4.61	**C***fad*8	−3.59	**C***pad*8	−4.39
C*bad*9	−4.98	**C***mad*9	−4.23	**C***fad*9	−4.01	**C***pad*9	−4.72
C*bad*10	−4.79	**C***mad*10	−4.9	**C***fad*10	−4.26	**C***pad*10	−4.47
C*bad*11	−4.6	**C***mad*11	−4.94	**C***fad*11	−4.14	**C***pad*11	−4.34
C*bad*12	−4.41	**C***mad*12	−4.13	**C***fad*12	−4.11	**C***pad*12	−4.34
C*bad*13	−4.41	**C***mad*13	−4.22	**C***fad*13	−4.06	**C***pad*13	−4.38
C*bad*14	−4.07	**C***mad*14	−3.83	**C***fad*14	−3.88	**C***pad*14	−4.43
C*bad*15	−4.43	**C***mad*15	−4.21	**C***fad*15	−4.16	**C***pad*15	−4.43
C*bad*16	−4.62	**C***mad*16	−4.67	**C***fad*16	−3.56	**C***pad*16	−4.28
C*bad*17	−5.03	**C***mad*17	−4.91	**C***fad*17	−3.75	**C***pad*17	−4.62

Table 5 $r^2_{m(\text{test})}$ obtained from MLR of ΔG_{calc} as a function of descriptors considered for each benzazole family

Considering	Benzimidazole	Benzothiazole	Benzoxazole
All series ($n = 68$)	$r^2_{m(\text{test})} = 0.2342$	$r^2_{m(\text{test})} = 0.1948$	$r^2_{m(\text{test})} = 0.3021$
bad series ($n = 17$)	$r^2_{m(\text{test})} = 0.7445$	$r^2_{m(\text{test})} = 0.8646$	$r^2_{m(\text{test})} = 0.9968$
mad series ($n = 17$)	$r^2_{m(\text{test})} = 0.8501$	$r^2_{m(\text{test})} = 0.9734$	$r^2_{m(\text{test})} = 0.9968$
fad series ($n = 17$)	$r^2_{m(\text{test})} = 0.9968$	$r^2_{m(\text{test})} = 0.9929$	$r^2_{m(\text{test})} = 0.9430$
pad series ($n = 17$)	$r^2_{m(\text{test})} = 0.7705$	$r^2_{m(\text{test})} = 0.8529$	$r^2_{m(\text{test})} = 0.9771$

rotatable bonds (N_B), polar surface area (*PSA*), molecular weight (*MW*), the partition coefficient (log *P*) and the solubility coefficient (log *S*).

The values obtained for these physicochemical properties of the ligands show that the best candidate is compound **B***fad*12, a benzothiazole derivative with a score of 93.33 %, which can be compared to **B***bad*9 with a score of 66.67 %. In the case of compound **B***fad*12, all of the carbons are sp^2, with the exception of an sp^3 methyl group. Additionally, the hydrocarbon chain at the C2 position is shorter (3 carbons) and is an α, β-unsaturated system that confers rigidity and extension of the conjugation, reducing its degrees of freedom. In the case of **B***bad*9, all of the carbons in the benzazole moiety are sp^2 without exception. At the C2 position, this compound has a chain with sp^3, which gives rise to greater freedom.

These results demonstrate that molecular modeling and docking simulations are not sufficient for molecular screening. It is necessary to take several other factors into account, including molecular geometry, lipophilicity and electronic density. These parameters were evaluated for the test compounds of the present study and compared to the values of the compounds *RefI, RefII, RefIII, RefIV,* ***C****fad3* and ***C****fad5* reported in the literature (86.67, 66.67, 70.0, 66.67, 83.33 and 83.33 %, respectively) (Flores *et al.*, 2013). Besides the relatively low score, compared to **B***fad*12, most of the compounds taken from the literature had fragments in their structure that act as irritants, and thus are potentially mutagenic and tumorigenic, and/or lead to reproductive malformations. For all compounds, the aforementioned parameters are shown in the Supplementary information.

QSAR study

The purpose of applying a QSAR method is to establish models that can improve our conception of molecular

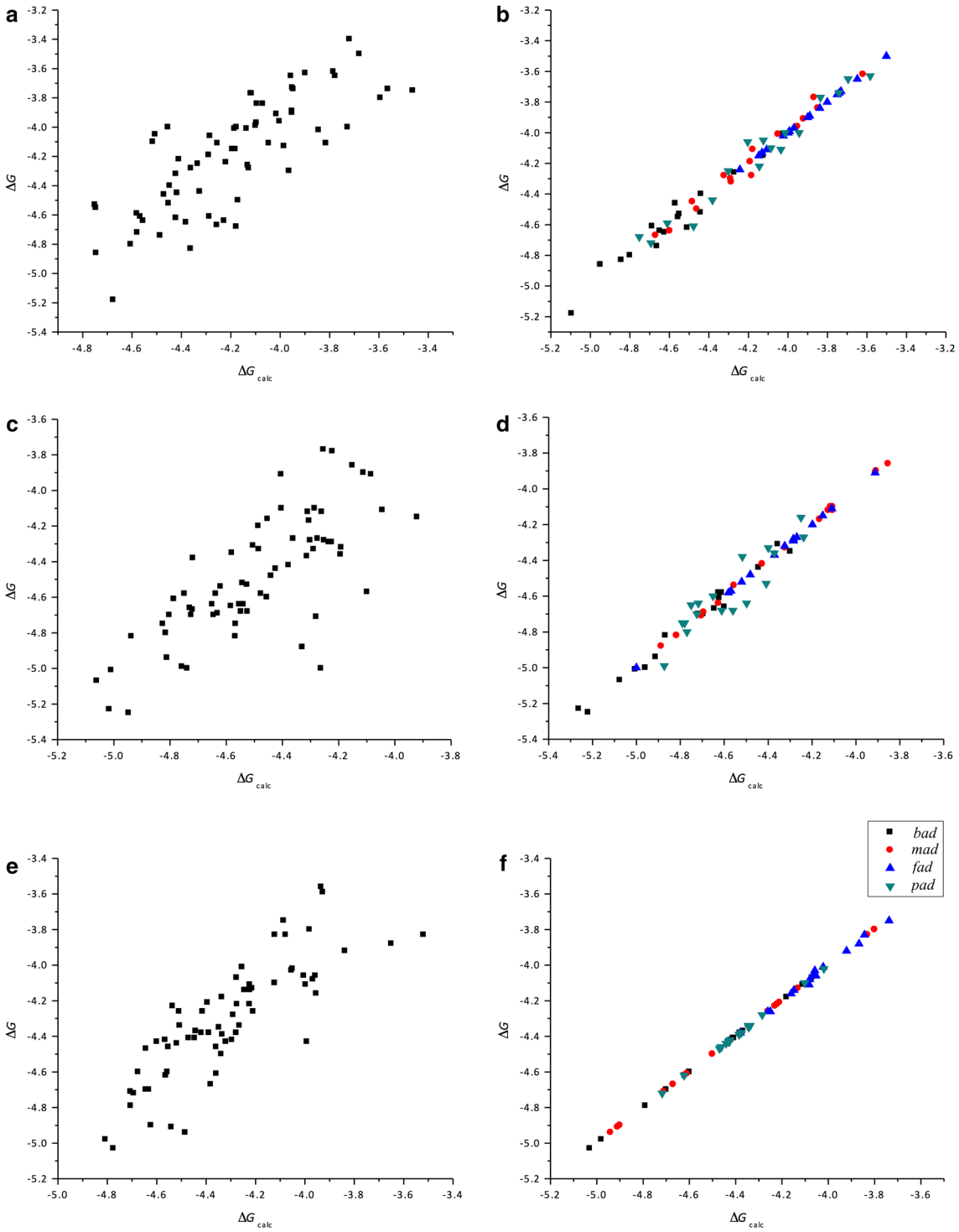

Fig. 1 Graph for the benzimidazole derivatives: **a** considering the four series together ($n = 68$), and **b** considering each individual series ($n = 17$). For the benzothiazole derivatives: **c** considering the four series together and **d** considering each individual series. For the benzoxazole derivatives: **e** considering the four series together and **f** considering each individual series. The *abscissa axis* represents ΔG calculated from physicochemical parameters, and the *ordinate axis* represents ΔG obtained by docking simulation

recognition based on behavioral data. Using physicochemical descriptors through a QSAR study in order to explain the molecular recognition obtained by docking simulations is a strategy that has established correlations with high predictive power in other studies (Correa *et al.*, 2014; Zekri *et al.*, 2009). This strategy has also been

Table 6 Molecular physicochemical properties for **BT1**, **BT2** and **BT3** ligands

Compound	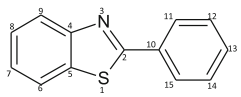	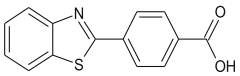	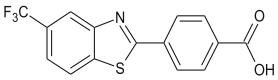
	BT 1	**BT2**	**BT3**
ΔG (Kcal/mol)	−4.35	−5.08	−4.93
MW (g/mol)	211.0	255.29	323.29
Log *P*	4.45	3.97	4.73
Log *S*	−3.18	−3.19	−3.97
PSA	12.89	50.191	50.19
N_B	1	2	3
N_{hba}	1	3	3
N_{hbd}	0	1	1
M	0	0	0
T	Medium	Medium	0
I	Medium	Medium	0
RE	0	0	0

ΔG enzyme-ligand *binding energy*, *Log P partition coefficient*, *Log S* solubility coefficient, *PSA* polar surface area, *MW* molecular weight, N_{hba} number of hydrogen bond acceptors, N_{hbd} number of hydrogen bond donors, N_B number of rotatable bonds, *M* mutagenic, *T* tumorigenic, *I* irritant, *RE* reproduction effects

employed to explain biological activity and mechanisms of action, or to modulate receptor–ligand molecular recognition (Zhang *et al.*, 2013; Voss *et al.*, 2014). For this purpose, quantum parameters were obtained from DFT calculations at the B3LYP/6-31G(*d*) level. The parameters taken into account for the QSAR study were the energy of the frontier molecular orbitals (E_{HOMO} and E_{LUMO}), the difference in energy between orbitals (*gap*), dipolar momentum (μ), molecular volume (V_M), electronegativity (χ), absolute hardness (η) and hydrophilicity (ω). Also considered was the electrostatic potential (*EP*) for nitrogen (N), sulfur (S) or oxygen (O) substituents, or the nitrogen atom with a double bond. The atomic charges of the N=C − X fragment (X = N, S or O) were obtained by employing the Merz-Singh-Kollman population analysis. Other descriptors considered were N_{hba}, N_{hbd}, N_B, *PSA*, *MW,* log *P*, log *S*, molar refractivity (*MR*), polarizability (α) and hydration energy ($E_{Hydration}$). Finally, each family (benzimidazole, benzothiazole and benzoxazole) includes four series of 17 compounds with differences in the chain length and the configuration of the double bond at the C2 substituent: *bad*, *mad*, *fad* and *pad*. To carry out the QSAR for each of the four series of the three families, the 17 compounds were separately analyzed by multiple linear regression (MLR), for a total of 204 compounds (see Table 5). The data for these parameters and the equations are included in supplementary information.

For the benzimidazole derivatives, the $r^2_{m(test)}$ value is acceptable when considering each series (*bad*, *mad*, *fad* or *pad*) separately. The most precise correlation was found with the *fad* series, which had an $r^2_{m(test)}$ value of 0.9968. However, when an entire family is considered (68 compounds), the $r^2_{m(test)}$ values have no correlation. This is particularly true when substituting α,β-unsaturated moieties in *trans* configuration at C2, which decreases freedom and gives rise to an extension of the conjugation. Additionally, in these compounds the methyl group increases lipophilicity. This information suggests that docking studies are insufficient for selecting the best compound and that other physical–chemical properties must be taken into account to improve the results (Fig. 1a, b).

For benzothiazole derivatives, there was a very low correlation when including the whole family (all four series) ($r^2_{m(test)} = 0.1948$). The best correlation was found with the sulfur substituent, where the $r^2_{m(test)}$ value for the *bad* series was 0.8656, for the *mad* series 0.9734, and for the *pad* series 0.8529 (Fig. 1c, d).

For the benzoxazole family, the $r^2_{m(test)}$ value showed the best correlation independently of whether the C2 substituent was saturated or unsaturated, or whether or not the configuration had a double bond Fig. 1e, f).

The in silico results suggest greater affinity between TcTIM and the proposed ligands whose substituent at the C2 position has an sp^2 carbon. Additionally, substituting

Table 7 The interactions involved in the ligand–enzyme complex, formed by the ligands **BT1**, **BT2**, **BT3** and **B***fad*12 and the amino acid residues of chain A or B of TIM

	B*fad*12	**BT1**	**BT2**	**BT3**
ΔG	−4.29	−4.35	−5.08	−4.93
A:Ile69	•	•	•	•
A:Thr70	•	•	•	•
A:Arg71	•[1]	•	•[1]	•[1]
A:Phe75		•[2]	•[2]	•[2]
A:Tyr103	•		•[2]	•[2]
A:Gly104	•		•	•
A:Glu105	•	•	•	•
A:Ile109	•		•	•
A:Lys113		•		•
B:Tyr102	•[2]	•[2]	•[2]	•[2]
B:Tyr103	•[2]	•[2]	•[2]	•[2]
B:Gly104				•

The binding energy (ΔG) is in Kcal/mol. The point (•) indicates that there is interaction with the amino acid residue; superscript one ([1]) indicates that the amino acid has hydrogen bond interactions with the ligand; superscript two ([2]) indicates that the amino acid has π–π interactions with the ligand

the NH fragment in position 1 with a sulfur atom gave fitting correlations for the series with unsaturated systems. However, in the case of the benzoxazoles, it was not possible to see any difference between any of the four series. Despite the good correlation in $r^2_{m(\text{test})}$ values, their affinity energies for TcTIM were lower than those of the other two families. The physicochemical properties evaluated herein indicate a high probability that the benzothiazole derivatives could be effective drugs for treatment of *T. cruzi*.

Compounds proposed for synthesis and biological study

The three compounds with the best score did not have an excellent ΔG value, indicating a less than desirable ligand–receptor affinity. However, these three compounds were all from the benzothiazole family. Therefore, we took the one with the best ΔG value as the lead compound to form three new compounds. This lead compound was a benzothiazole with the fad substituent at C2 and the methyl group at C6.

To form **BT1** (*2-phenyl-1,3-benzothiazole*), we added a benzyl group at C2 because the best 3 compounds all had an sp^2 geometry for all the carbons. To form **BT2** (*4-(1,3-benzothiazol-2-yl)benzoic acid*), we started with **BT1** as the new lead compound and added a carboxylic group in the *para* position of the benzyl group in order to extend the sp^2 hybridization carbons, because all of the recognition between the two chains (A and B) of TIM is by π–π interactions. To form **BT3** (*4-[5-(trifluoromethyl)-1,3-benzothiazol-2-yl]benzoic acid*), we started with **BT2** as the new lead compound and added a trifluoromethyl group (an electron-withdrawing group, $\sigma_m = 0.43$) at C6 instead of the methyl group of **B***fad*12 in order to obtain a better log *P* (Table 6). Thus **BT3** is notably more lipophilic than **BT1** and **BT2**, enabling it to pass through lipidic membranes to reach *T. cruzi*, which is an intracellular parasite. Organic compounds that contain fluoride groups have good physicochemical properties in regard to biological activity (Pursor *et al.*, 2008; Filler and Saha, 2009), improving lipophilicity and increasing the velocity of diffusion through cellular membranes (Bhavanarushi *et al.*, 2014). Hence, **BT3** is an isostere of the **B***fad*12 compound and contains an unsaturated system at the C2 position.

Of these three compounds, **BT1** and **BT2** had problems with toxicity (based on the toxicological database for several different drugs). **BT3**, however, was acceptable in respect to this parameter. This clearly shows that the trifluoromethyl group is particularly important for better effects. Additionally, the ΔG is much better for **BT3** than **BT1** or **BT2**. On the other hand, molecular recognition data obtained from docking simulations show that the affinity for TcTIM increases with **BT3** as opposed to its isostere, **B***fad*12. It seems that this is due to the incorporation of one more aromatic ring at the C2 position, which interacts with the aromatic cluster residues present in the TcTIM dimer interface. This idea is in agreement with a previous report (Espinoza and Trujillo, 2005). The consensus binding site found for **B***fad*12, **BT1, BT2** and **BT3** corresponds to the following amino acid residues of chain A or B of TIM: A:Ile69, A:Thr70, A:Arg71, A:Phe75, A:Tyr103,

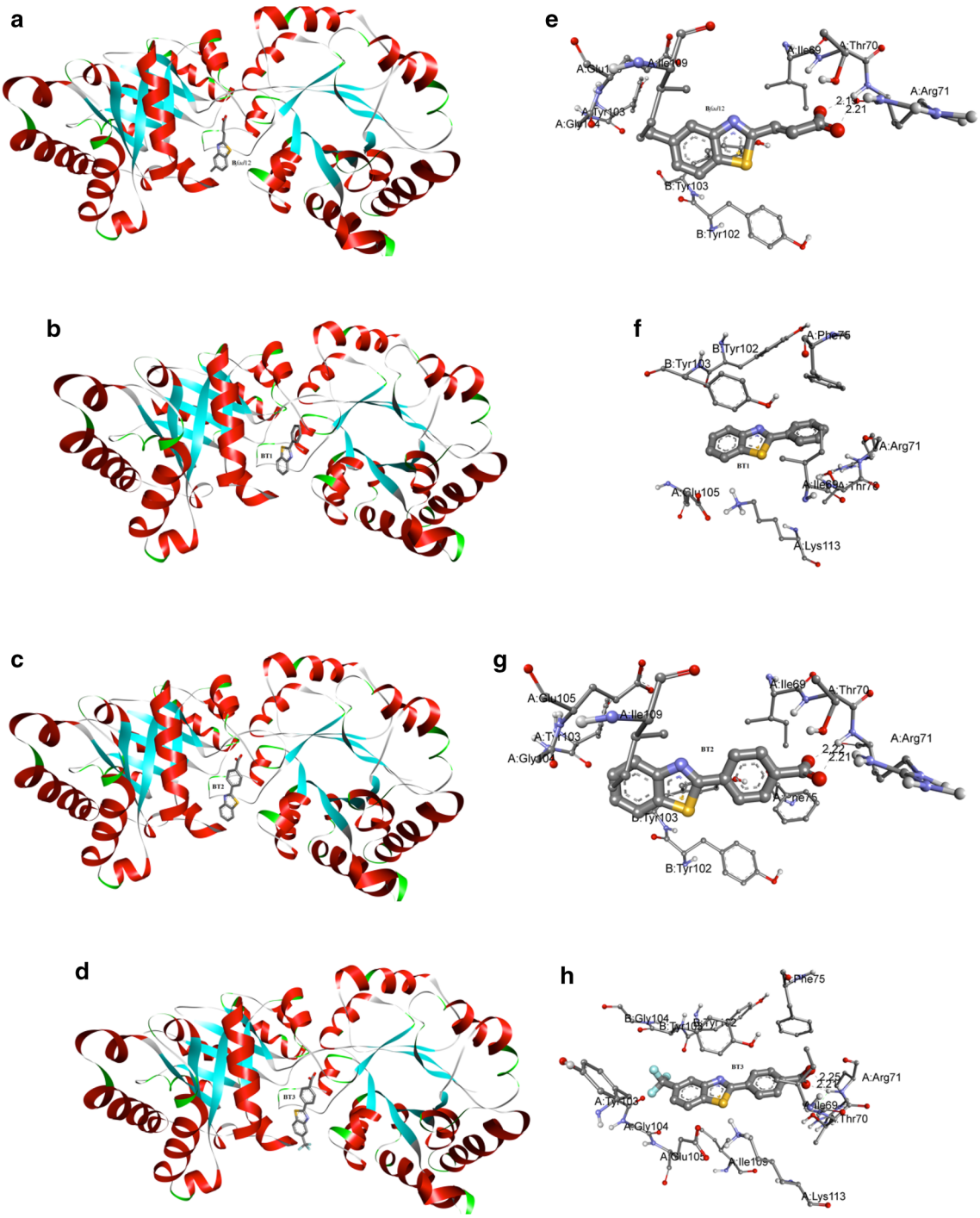

Fig. 2 Binding mode on TcTIM obtained by docking simulation. **a**–**d** Stereoview of the ligand binding sites located at the TcTIM interface. **e**–**h** Schematic representation of the binding site for **B***fad*12 (**e**), **BT1** (**f**), **BT2** (**g**) and **BT3** (**h**). *Dotted lines* represent hydrogen bond interactions and distances are in Å

A:Gly104, A:Glu105, A:Ile109, A:Lys113, B:Tyr102, B:Tyr103 and B:Gly104. The interactions involved for each complex are summarized in Table 7 and shown in Fig. 2. Hence, **BT1**, **BT2** and **BT3** were synthesized, evaluated in vitro with *T. cruzi* and compared with the results found with **C***fad*3 and **C***fad*5, previously reported to

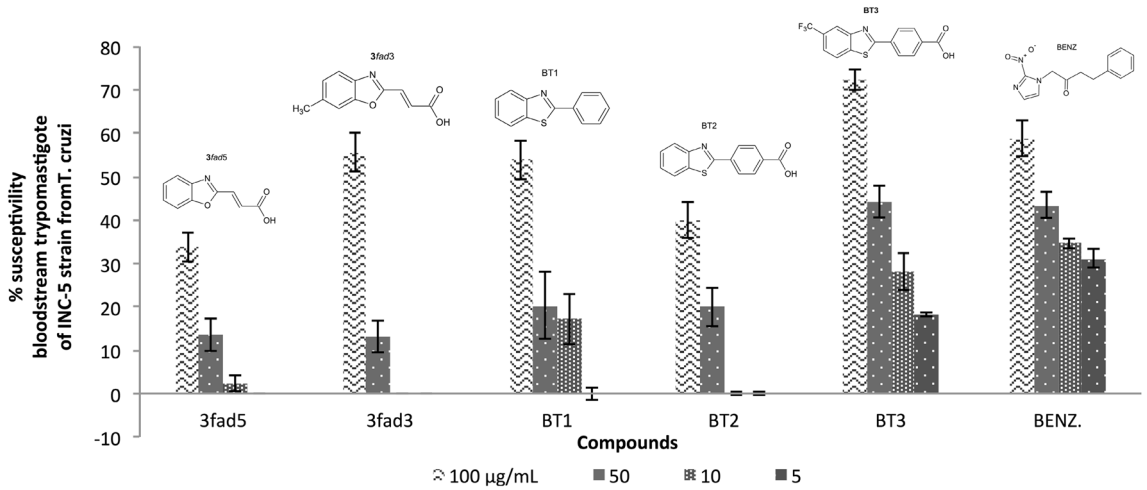

Fig. 3 Trypanocidal activity of compounds **C***fad*5, **C***fad*3, **BT1**, **BT2**, **BT3** and Benznidazol (BZN), based on the percentage of lysis of the INC-5 strain of *T. cruzi* that was isolated from the blood of Chagas patients

be trypanocides. **C***fad*3 and **C***fad*5 were compared with benznidazol, but did not prove to have better trypanocidal activity (Flores *et al.*, 2013).

Trypanocidal activity

After synthesis and characterization, **BT1**, **BT2** and **BT3** were tested in vitro for their biological activity against the INC-5 strain of *T. cruzi*, isolated from the blood of patients with chronic Chagas disease. The concentrations of the test compounds were 5, 10, 50 and 100 µg/mL, and the results showed that all the compounds have trypanocidal activity. However, only compound **BT3**, beginning at the concentration of 50 µg/mL, proved to have greater trypanocidal activity than the reference compound benznidazol (BZN) (72.3 % versus 58.9 %; Fig. 3).

Conclusion

Regarding the biological activity of benzoxazoles **C***fad*3 and **C***fad*5, the in vitro and in silico results are in agreement with each other and with previous reports, thus validating the current model. The $r^2_{m(\text{test})}$ values of multiple linear regression for the QSAR studies found an acceptable correlation for the benzothiazoles, **BT1**, **BT2** and **BT3**, supporting the idea that the substitution at C2 with a unsaturated system tends to favor molecular recognition with TcTIM. For **BT3**, the substitution at the C2 position with an aromatic ring increased affinity for the cluster of aromatic residues present at the interface of the dimeric monomers of TcTIM. The data obtained from the docking studies show that affinity for TcTIM is greater with **BT3** than with its isostere **B***fad*12 and that the isosteric replacement of CH_3 by CF_3 improved the interaction with the receptor as well as the lipophilicity of the compound, thus allowing **BT3** to diffuse more rapidly through cellular membranes and reach its pharmacological target. Finally, **BT3** proved to be a better trypanocide than **BT1** and **BT2**, in agreement with predictions, and also better than the currently used drug on the market for the treatment of Chagas disease, benznidazol. In general, **BT3** fulfills the requirements proposed by Lipinski and Veber for compounds to be considered as new drugs. **BT3** should certainly be of interest for further testing in animal models and/or clinical trials, especially when considering that there is currently no effective treatment for Chagas disease.

Acknowledgments We are grateful to the Consejo Nacional de Ciencia y Tecnología (CONACyT), Comisión de Operación y Fomento de Actividades Académicas del Instituto Politécnico Nacional (COFAA-IPN) for financial support and CNMN-IPN for experimental support. We thank Bruce Allan Larsen for proofreading this manuscript and Ariana Lucas for her contribution in the style of the figures.

Compliance with ethical standards

Conflict of interest The authors confirm that the article content has no conflict of interest.

References

Akaike H (1974) A new look at the statical model identification. IEEE Trans Autom Control 19:716–723

Alvarez G, Aguirre B, Varela J, Cabrera M, Merlino A, López GV, Lavaggi ML, Porcal W, Di Maio R, González M, Cerecetto H, Cabrera N, Pérez R, de Gómez-Puyou MT, Gómez-Puyou A (2010) Massive screening yields novel and selective *Trypanosoma cruzi* triosephosphate isomerase dimer-interface-irreversible inhibitors with anti-trypanosomal activity. Eur J Med Chem 45:5767–5772

Banner D, Bloomer A, Petsko G, Phillips D, Pogson C, Willson I, Conan P, Furth A, Milmar J, Offord R, Priddle J, Waley S (1975) Structure of chicken muscle triose phosphate isomerase determined crystallographically at 2.5 angstrom resolution using amino acid sequence data. Nature 19(255):609–614

Bhavanarushi S, Kanakaiah V, Bharath G, Gangagnirao A, Vatsala J (2014) Synthesis and antibacterial activity of 4,4′-(aryl or alkyl methylene)-bis(1H-pyrazol-5-ol) derivatives. Med Chem Res. doi:10.1007/s00044-013-0623-3

Correa J et al (2014) QSAR, docking, dynamic simulation and quantum mechanics studies to explore the recognition properties of cholinesterase binding sites. Chem Biol Interact 209:1–13

Dassault Systèmes BIOVIA (2015) Discovery Studio Modeling Environment, Release 4.5. Dassault Systèmes, San Diego

Díaz DL et al (2011) In vitro and in vivo trypanocidal activity of some benzimidazole derivatives against two strains of *Trypanosoma cruzi*. Acta Trop. doi:10.1016/j.actatropica.2011.12.009

Espinoza LM, Trujillo JG (2004) Exploring the possible binding sites at the interface of triosephosphate isomerase dimer as a potential target for anti-trypanosomal drug design. Bioorg Med Chem Lett 14(12):3151–3154

Espinoza LM, Trujillo JG (2005) Structural considerations for the rational design of selective anti-trypanosomal agents: the role of the aromatic clusters at the interface of triosephosphate isomerase dimer. Biochem Biophys Res Commun 25 328(4): 922–928

Espinoza LM, Trujillo JG (2006) Toward a rational design of selective multi-trypanosomatid inhibitors: a computational docking study. Bioorg Med Chem Lett 16(24):6288–6292

Espinoza LM, Wong C, Trujillo JG (2010) Tyr74 is essential for the formation, stability and function of *Plasmodium falciparum* triosephosphate isomerase dimer. Arch Biochem Biophys 494(1):46–57

Filler R, Saha R (2009) Fluorine in medicinal chemistry: a century of progress and a 60-year retrospective of selected highlights. Future Med Chem 1(5):777–791

Flores CA, Cuevas RI, Correa J, Beltrán HI, Padilla II, Farfán JN, Nogueda B, Trujillo JG (2013) Synthesis and theoretic calculations of benzoxazoles and docking studies of their interactions with triosephosphate isomerase. Med Chem Res 22:2768–2777

Frisch MJ et al (2003) Gaussian 03, Revision A.1. Gaussian Inc, Pittsburgh

Garza G, Cabrera N, Saavedra E, Tuena de Gomez-Puyou M, Ostoa P et al (1998) Sulfhydryl reagent susceptibility in proteins with high sequence similarity—triosephosphate isomerase from *Trypanosoma brucei*, *Trypanosoma cruzi* and *Leishmania mexicana*. Eur J Biochem 253:684–691

Guha R, Jurs PC (2005) Determining the validity of QSAR model—a classification approach. J Chem Inf Model 45:65–73

Hansch C, Leo A, Taft RA (1991) Survey of hammett substituent constants and resonance and field parameters. Chem Rev 91(2):165–195

Humphrey W, Dalke A, Schulten K (1996) VMD: visual molecular dynamics. J Mol Graph 14:33–38

Knowles JR (1991) Enzyme catalysis, not different, just better. Nature 350:121–124

Lipinski CA, Lombardo F, Dominy BW, Feeney PJ (2001) Experimental and computational approaches to estimate solubility and permeability in drug discovery and development settings. Adv Drug Deliv Rev 46:3–26

Lolis E, Petsko GA (1990) Crystallographic analysis of the complex between triosephosphate isomerase and 2-phosphoglycerate at 2.5-Å resolution implications for catalysis. Biochemistry 29:6619–6625

Maldonado E, Soriano M, Moreno A, Cabrera N, Garza G, De Gomez-Puyou T, Gomez A, Perez R (1998) Differences in the intersubunit contacts in triosephosphate isomerase from two closely related pathogenic trypanosomes. J Mol Biol 283:193–203

Marin JÁ, Cunha E, Maciel BC, Simoes MV (2007) Pathogenesis of chronic Chagas heart disease. Circulation 115:1109–1123

Molisnpiration Cheminformatics (2015). http://www.molinspiration.com/cgi-bin/properties

Morris GM, Goodsell DS, Halliday RS, Huey R, Hart WE, Belew RK, Olson AJ (1998) Automated docking using a Lamarckian genetic algorithm and an empirical binding free energy function. J Comput Chem 19:1639–1662

Olivares V, Rodríguez A, Becker I, Berzunza M, García J et al (2007) Perturbation of the dimer interface of triosephosphate isomerase and its effect on *Trypanosoma cruzi*. PLoS Negl Trop Dis 1(1):e01. doi:10.1371/journal.pntd.0000001

Organización Panamericana de la Salud (2006) Estimación cuantitativa de la enfermedad de Chagas en las Américas (Documento OPS/HDM/CD/425.06.). Washington (DC), EUA. Washington (DC): OPS

Osiris Property Explorer (2015). http://www.organic-chemistry.org/prog/peo/

Phillips JC, Braun R, Wang W, Gumbart J, Tajkhorshid E, Villa E, Chipot C, Skeel RD, Kalé L, Schulten K (2005) Scalable molecular dynamics with NAMD. J Comput Chem 26(16):1781–1802

Pursor S, Moore PR, Swallow S, Gouverneur V (2008) Fluorine in medicinal chemistry. Chem Soc Rev 37:320–330

Rassi A Jr, Rassi A, Marin JÁ (2010) Chagas disease. Lancet 375:1388–1402

Romo A, Téllez A, Yépez L, Hernández F, Hernández A, Castillo R (2011) The design and inhibitory profile of new benzimidazole derivatives against triosephosphate isomerase from *Trypanosoma cruzi*: a problem of residue motility. J Mol Graph Model 30:90–99

Roy PP, Roy K (2008) On some aspects of variable selection for partial least squares regression models. QSAR Comb Sci 27:302–313

Roy PP, Paul S, Mitra I, Roy K (2009) On two novel parameters for validation of predictive QSAR models. Molecules 14: 1660–1701

Saab G, Juárez R, Osuna J, Sánchez F, Soberón X (2011) Different strategies to recover the activity of monomeric triosephosphate isomerase by directed evolution. Protein Eng 14:149–155

Sanner MF (1999) Python: a programming language for software integration and development. J Mol Graph Mod 17:57–61

SPSS for windows (1999) Version 10.05. SPSS Inc, Bangalore, India

Trujillo JG et al (2004) The E and Z isomers of 3-(benzoxazol-2-yl)prop-2-enoic acid. Acta Crystallogr C 60(Pt 10):o723–o726

Veber DF, Johnson SR, Cheng HY, Smith BR, Ward KW, Kopple KD (2002) Molecular properties that influence the oral bioavailability of drug candidates. J Med Chem 45:2615–2623

Verlinde CL, Hannaert V, Blonski C, Willson M, Périé JJ, Fothergill LA, Opperdoes FR, Gelb MH, Hol WG, Michels PA (2001) Glycolysis as a target for the design of new anti-trypanosome drugs. Drug Resist Updates 4:1–14

Voss C et al (2014) α-Keto phenylamides as P1′-extended proteasome inhibitors. Chem Med Chem 9:2557–2564

Weekes AA et al (2011) An efficient synthetic route to biologically relevant 2-phenylbenzothiazoles substituted on the benzothiazole ring. Tetrahedron 67:7743–7747

World Health Organization (2015) Chagas disease (American trypanosomiasis). http://www.who.int/mediacentre/factsheets/fs340/en/index.html. Accessed 13 Jan 2015

Xu J, Wang L, Zhang H, Shen X, Liang G (2012) Quantitative structure property relationship studies on free-radical polymerization chain-transfer constants for styrene. J Appl Polym Sci 123:356–364

Zekri O et al (2009) Role of aromatic substituents on the antiproliferative effects of diphenyl ferrocenyl butene compounds. Dalton Trans 22:4318–4326

Zhang HJ et al (2013) Enzymatic synthesis of theanine with *Escherichia coli* γ-glutamyltranspeptidase from a series of γ-glutamyl anilide substrate analogues. Biotechnol Bioprocess Eng 18:358–364

Zomosa V, Hernández G, Reyes H, Martínez E, Garza G, Pérez R, Tuena De Gómez-Puyou M, Gómez A (2003) Control of the reactivation kinetics of homodimeric triosephosphate isomerase from unfolded monomer. Biochemistry 42:3311–3318